

Thermoeconomic assessment and optimization of wells to flash–binary cycle using pure R601 and zeotropic mixtures in the Sibayak geothermal field

Felix Pratama^{a,b}, Nadhilah Reyseliani^{a,b}, Ahmad Syauqi^{a,b}, Yunus Daud^{a,c},
Widodo Wahyu Purwanto^{a,b,*}, Praswasti P.D.K. Wulan^b, Akhmad Hidayatno^{a,d}

^a Sustainable Energy Systems and Policy Research Cluster, Universitas Indonesia, Depok, 16424, Indonesia

^b Department of Chemical Engineering, Faculty of Engineering, Universitas Indonesia, Depok 16424, Indonesia

^c Geothermal Research Center (GRC), Faculty of Mathematics and Natural Science, Universitas Indonesia, Depok, 16424, Indonesia

^d Department of Industrial Engineering, Faculty of Engineering, Universitas Indonesia, Depok 16424, Indonesia

ARTICLE INFO

Keywords:

Flash-binary cycle
Optimization
Pipelines
Sibayak geothermal field
Zeotropic mixtures

ABSTRACT

In this study, a flash–binary cycle is proposed with the pressure and energy loss from well to power plant are quantified in the Sibayak geothermal field. The reservoir deliverability curve is simulated using WellSim. The cycle is simulated with various zeotropic mixtures as the working fluid of the organic Rankine cycle (ORC) using Honeywell UniSim Design and optimized in terms of maximum NPV and maximum power output using Genetic Algorithm. The optimization shows that pure R601 as the ORC working fluid resulting USD 29,224,825 NPV and 27.88 MW power equivalent to 6.23 % exergy efficiency improvement compared to single flash. The integration system shows 0.73–0.93 bar pressure loss and 0.53 MW energy loss due to the consideration of pipeline system that is equal to 0.23 Cents/kWh electricity price overestimation.

1. Introduction

Indonesia's electricity requirements are still being primarily fulfilled by fossil fuels. Although fossil-based energy is promising from the aspect of process efficiency, the burning of fossil fuels leads to a large amount of greenhouse gas emissions; moreover, fossil fuel sources are becoming scarce (Prananto et al., 2018). A promising solution to address this problem is the use of renewable energy. Geothermal energy, as one of the most mature renewable energies, is considered as an attractive source (Shokati et al., 2015).

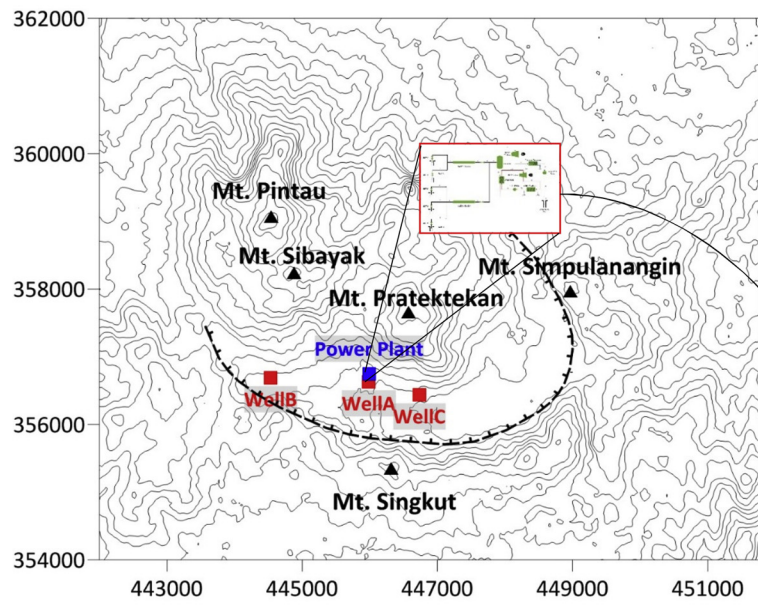
The majority of geothermal power plants used in Indonesia is using single-flash cycle systems (Pambudi, 2018; Mohammadzadeh Bina et al., 2018). One of the geothermal fields that use this cycle is the Sibayak geothermal field. This field which located in North Sumatra, Indonesia and classified as a volcanic geothermal system with a liquid-dominated reservoir and high calcite concentration, has proven reservoir reserves of 40 MWe (Sinaga and Manik, 2018). The single-flash cycle used in the Sibayak geothermal field has a power output of 20 MWe (Siregar, 2004). The main problem with this cycle is that saturated liquid that comes out from separator, or brine, still contains high energy. Based on the exergy analysis conducted by (Pambudi et al., 2014) and (Jalilinasrabady et al., 2012), show that exergy loss from brine reaches 17.98 % (10.70 MW) and 41.44 % (46.33 MW) of the total

exergy input. Several studies have been conducted to maximize energy utilization from geothermal energy by adding bottoming cycles that flash a large amount of brine to lower pressure. Yari (2010) compared the performance of different geothermal power plant configurations (single-flash, double-flash, flash–binary, and binary geothermal plants) based on energy and exergy analysis, and the results showed that a flash–binary cycle with R123 as the organic Rankine cycle (ORC) working fluid achieved maximum exergy efficiency by 48.28 %. Another related research had been conducted and concluded that the flash-binary system has the highest exergy efficiency among others (Aali et al., 2017). (Pambudi et al., 2018) showed that the double flash system resulting the highest energy and exergy efficiency and lowest investment cost compare to other cycles. (Mokarram and Mosaffa, 2018) showed that when an enhanced double flash/modified Kalina cycle is used, generated power increases by 6 % compare to the basic cycle under the optimum operating condition.

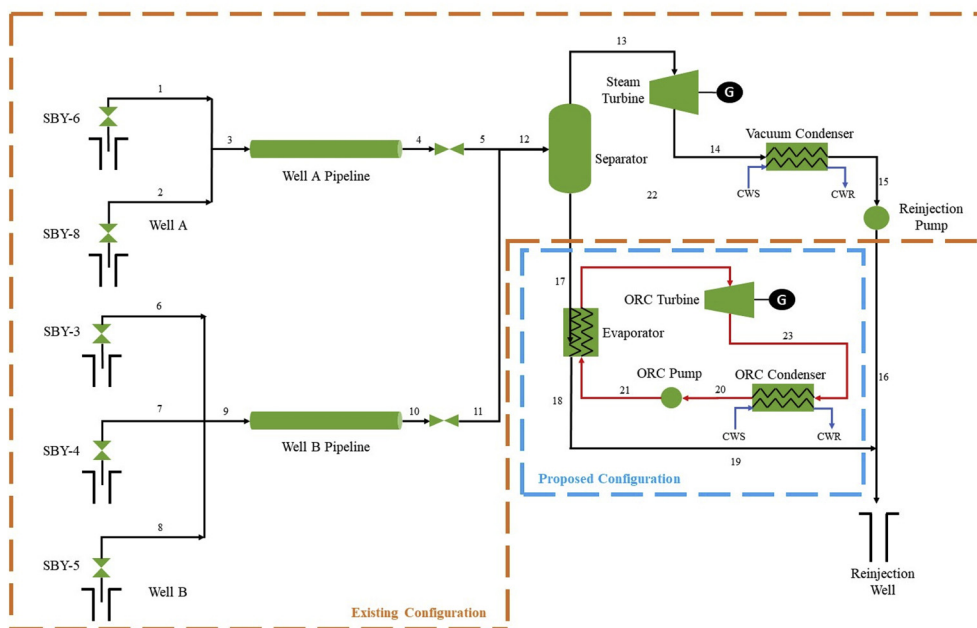
To implement the bottoming cycle in the geothermal power plant, it is necessary to choose the optimized working fluid. The selection of the working fluid for the ORC is very important in designing system process (Kolahi et al., 2018). By optimizing the exergy efficiency and cost, (Aali et al., 2017) found that using R141b reduce the cost by up to 3 % compared to other working fluids, and increase the exergy efficiency by 10 %. (Zeyghami, 2015) showed that for the combined flash-binary

* Corresponding author at: Sustainable Energy System and Policy Research Cluster, Universitas Indonesia, Depok, 16424, Indonesia.

E-mail addresses: widodo@che.ui.ac.id (W.W. Purwanto), wulan@che.ui.ac.id (P.P.D.K. Wulan), akhmad@eng.ui.ac.id (A. Hidayatno).



(a)



(b)

Fig. 1. (a) Sibayak geothermal field; (b) schematic diagram of existing and proposed process flow from wells to power plant.

cycle with R-152a, butane and cis-butane as secondary working fluids, resulting in the overall exergy efficiency of 0.48, 0.55 and 0.58 for geofluid at temperature 150, 200 and 250 °C, respectively. Also, (Pasek et al., 2011) compared i-butane, n-butane, i-pentane, and n-pentane in terms of net power produced which are 2915.79, 3057.31, 3077.64, and 2793.85 kW, respectively. Meanwhile (Edrisi and Michaelides, 2013), discovered that pure hexane has the highest exergy efficiency of about 57.6 %. (Wang et al., 2013b, a) conducted an ORC performance evaluation and guided working fluid selection based on the heat source temperature. Based on this research, the pure working fluids used in this study are R600, R142b, butene, and R601.

Currently, zeotropic mixtures are proposed to be the working fluid of ORC. (Su et al., 2018) discovered that zeotropic mixtures R-600a/R-601a had lower energy and exergy efficiency compared to the pure R-601a. (Oyewunmi et al., 2017) stated that pure pentane is better than zeotropic mixtures of Hexane/Butane in terms of cost. Hence, the working fluid used in the bottoming cycle greatly affects the performance of a geothermal power plant. (Kolahi et al., 2018) discovered that mixture containing pentane is better in terms of maximizing total power output (increased by about 20 %) than pure fluids.

For a more integrative approach compared to previous studies that ignored the pressure drop in the piping system (Leveni et al., 2019; Wang et al., 2017), the system reviewed in this study is started from the reservoir to the power plant (well to power). The integration system needs to be considered and quantified due to losses in the piping system, especially for systems with relatively a long distance between geothermal and power plants. Moreover, the challenge for volcanic geothermal is the high content of calcite as impurities that can increase pressure drop. Another study that related to well to power in geothermal systems have been conducted by (Minoli et al., 2017). (Minoli et al., 2017) conducted an optimization to maximize the power output of the ORC, taking into account the existence of production wells. The distance from the power plant to the production wellhead is assumed to be close enough so that the pressure drop and heat loss of the geothermal fluid flowing from the production wellhead to the power plant is negligible. From the assumption, the operating pressure at the wellhead is set equal to the separator pressure. However, this assumption has not been quantified by other studies.

Therefore, the objectives of the present work are to propose a flash-binary cycle with ORC to increase the efficiency of the power plant cycle through energy utilization in brine and to quantify the pressure and energy loss in the pipeline system. The working fluid selection among pure fluid and the zeotropic mixture is determined by optimization in terms of maximizing NPV and power output value.

2. Methods

To simplify the system performance simulation in the present study, the assumptions are made as follow:

- 1 The process from production wells to power plant operates under steady-state conditions (Aali et al., 2017; Kolahi et al., 2018; Zhao and Wang, 2016; Mokarram and Mosaffa, 2018)
- 2 For calculation of the thermodynamic properties, the geothermal fluid is assumed to be pure water (Aali et al., 2017; Mokarram and Mosaffa, 2018; Su et al., 2018)
- 3 The pressure drop, heat loss, and changes in kinetic and potential energy in the power plant are neglected (Kolahi et al., 2018; Su et al., 2018).
- 4 The working fluids' and the mixtures' composition do not change during operation (Kolahi et al., 2018; Su et al., 2018).
- 5 The ambient temperature and pressure (dead state) at the Sibayak geothermal field are 291.15 K and 0.86 atm, respectively (Forecasts, 2019).

2.1. System description

Based on data from (Yunus Daud et al., 1999) and (Siregar, 2004), there are five active production wells in the Sibayak geothermal field (SBY-3, SBY-4, SBY-5, SBY-6, and SBY-8) with a total power output of ~20 MWe. Fig. 1a shows the wells and power plant located in the Sibayak geothermal field. The schematic diagram of the process flow from the wells to the power plant for simulation is shown in Fig. 1b. A two-phase geothermal fluid produced from the production wells is sent to the power plant using pipelines and throttled by a valve to lower pressure. Then, the geothermal fluid is separated into saturated steam and saturated liquid or brine in the separator. The saturated steam enters a steam turbine to produce electricity, while the brine enters an evaporator in the ORC system to release heat to evaporate the working fluid of the ORC. Expanded steam from the steam turbine is condensed and pumped back into the injection well. In the ORC system, the working fluid in a saturated liquid condition is pressurized by pumping it to a higher pressure. Then, the working fluid absorbs the heat from the brine in the evaporator until it reaches a saturated vapor condition. The working fluid is expanded in the ORC turbine to a lower pressure to produce electricity. The brine stream from the evaporator is injected back into the injection well.

The working fluid reviewed in this study are pure R601 and mixture of R600, R601, R142b, and butene. R601 is chosen for mixing with R600, R142b, and butene to obtain zeotropic mixtures. The utilization of zeotropic mixtures as a working fluid gives a temperature glide in the phase change that provides better temperature matching between the working fluid and the heat stream or cold stream. The better temperature matching also enables the cycle to achieve higher thermal efficiency and lower exergy destruction. Table 1 lists the characteristics of the working fluid candidates.

2.2. Wellbore simulation and validation

To obtain the deliverability curve for each well, in this study, the production wells are simulated using WellSim. The deliverability curve will be validated using the actual data (Siregar, 2004). The deliverability curve equations are used as input for pipelines and for the power plant simulation in Honeywell UniSim Design. Reservoir simulation results used for the well simulation are obtained from (Putra et al., 2014), while well production data, inclination, and depth are obtained from (Siregar, 2004), (Atmojo et al., 2019), and (Yunus Daud et al., 1999).

2.3. Pipeline system

The pipelines are designed properly to prevent slug flow, reduce heat losses, and reduce pressure drops in the geothermal fluid that flows through the pipelines. The pipeline was also designed to prevent the fluid velocity from exceeding its erosional velocity. A flowsheet for the simulation is shown in Fig. 2; the input parameters used in the simulation are listed in Table 2 (Zare and Mahmoudi, 2015; Vankeirsbilck et al., 2011; Ghasemian and Ehyaei, 2018).

Table 1
Properties of working fluids used in this study.

Fluid	Molecular mass (g/mol)	T_{bp} (°C)	T_{cr} (K)	P_{cr} (MPa)	ODP	GWP
R600	58.12	272.63	425.15	3.80	0	~20
R601	72.15	309.15	469.65	3.37	0	~20
R142b	100.49	263.85	410.35	4.12	0.065	2400
Butene	56.11	272.63	425.15	4.01	n.a.	n.a.

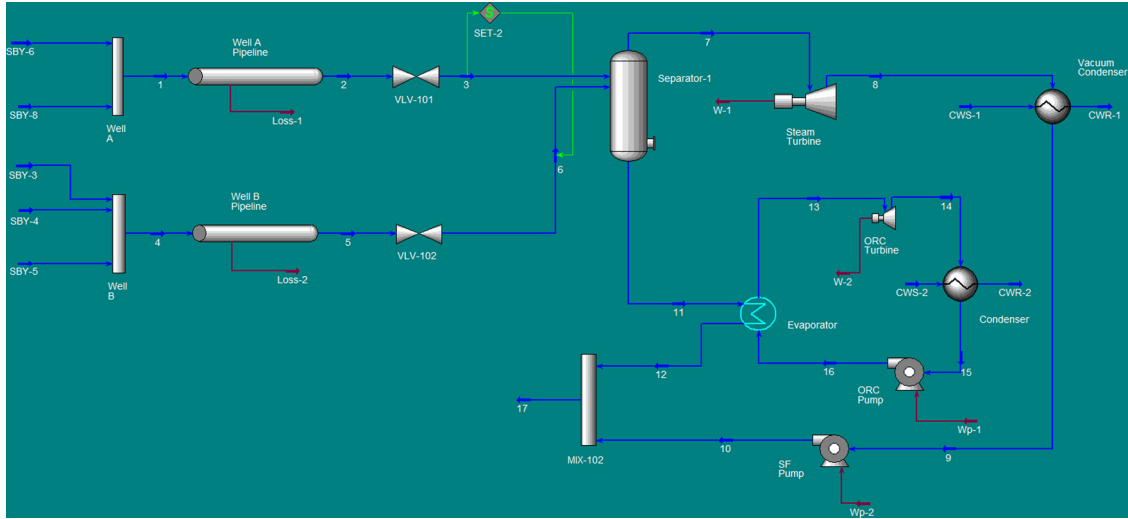


Fig. 2. Simulation flowsheet from wellhead to power plant.

Table 2
Input parameters for power plant cycle simulation.

Parameter	Value
Inlet temperature of cooling water (°C)	30
Outlet temperature of cooling water (°C)	40
Inlet pressure of cooling water (bar)	3
Evaporator pinch point temperature difference (°C)	10
Condenser pinch point temperature difference (°C)	10
Isentropic efficiency of turbine (%)	75
Isentropic efficiency of pump (%)	85

2.4. Thermo-economic analysis

Based on the assumptions that the system operates under steady-state conditions and the changes in kinetic and potential energy are neglected, the mass, energy, and exergy balances for each component of the system are expressed in Eqs. 1–3 (Yilmaz, 2018):

$$\sum \dot{m}_{in} = \sum \dot{m}_{out} \tag{1}$$

$$\dot{Q} - \dot{W} = \sum \dot{m}_{out} h_{out} - \sum \dot{m}_{in} h_{in} \tag{2}$$

$$\dot{E}_Q - \dot{W} = \sum \dot{m}_{out} e_{out} - \sum \dot{m}_{in} e_{in} + \dot{E}_D \tag{3}$$

The net power output produced by the power plant is calculated using Eq. 4.

$$\dot{W}_{Net} = \dot{W}_{T,SF} + \dot{W}_{T,ORC} - \dot{W}_{P,SF} - \dot{W}_{P,ORC} \tag{4}$$

The exergy rate from heat transfer (\dot{E}_Q) and specific exergy flow (e) are calculated using Eqs. 5 and 6.

$$\dot{E}_Q = \dot{Q} \left(1 - \frac{T_0}{T} \right) \tag{5}$$

$$e = h - h_0 - T_0 (s - s_0) \tag{6}$$

The energy efficiency (η_{th}) and exergy efficiency (η_{ex}) of the overall system are defined in Eqs. 7 and 8.

$$\eta_{th} = \frac{\dot{W}_{Net}}{m_1 (h_1 - h_0) + m_2 (h_2 - h_0)} \tag{7}$$

$$\eta_{ex} = \frac{\dot{W}_{Net}}{m_1 e_1 + m_2 e_2} \tag{8}$$

For the economic analysis, the NPV is chosen as the parameter for economic evaluation of the overall system. The NPV is expressed in Eq.

Table 3
Assumed parameters used in economic analysis.

Parameter	Unit	Value	Reference
Electricity price	USD/kWh	0.14	–
Fixed O&M	USD	1.5 % of C_{TPI}	Schuster et al. (2009)
Variable O&M	USD/kW	110	IRENA (2018)
Tax	USD	34 % of gross profit	Minister of Finance Decree Republic of Indonesia Number 90/PMK.02/2017
Interest rate	–	0.10	IRENA (2018)
Lifetime	years	25	IRENA (2018)
Capacity factor	–	0.90	IRENA (2018)

9.

$$NPV = \sum_{n=1}^N \frac{CF}{(1+i)^n} - C_{TCI} \tag{9}$$

the cash flow is calculated using Eq. 10.

$$CF = R - O\&M - Tax \tag{10}$$

where C_{TCI} is the total investment costs of the overall system, R is the revenue generated from electricity sales, $O\&M$ is the operation and maintenance costs, i is the interest rate, and N is the lifetime for economic evaluation. The assumed parameters used for the economic analysis are listed in Table 3. The investment costs of geothermal wells, pipelines, and equipment in the power plants are calculated using references from (Lukawski et al., 2014), (Quinlivan, 2009), and (Seider, 2004). The separator in the single-flash cycle is designed based on the work of (Zarrouk and Purnanto, 2015).

2.5. Optimization

The objective functions in this study are NPV and W_{Net} . Decision variables are wellhead pressure (P_A and WHP_B), separator pressure in the Single Flash cycle (P_{Sep}), and the mole fraction of R601 (x_{R601}). Mathematically, these can be written as shown in Eqs. 11 and 12.

$$\max NPV (WHP_A, WHP_B, P_{Sep}, x_{R601}) \tag{11}$$

and

$$\max W_{Net} (WHP_A, WHP_B, P_{Sep}, x_{R601}) \tag{12}$$

with boundary conditions

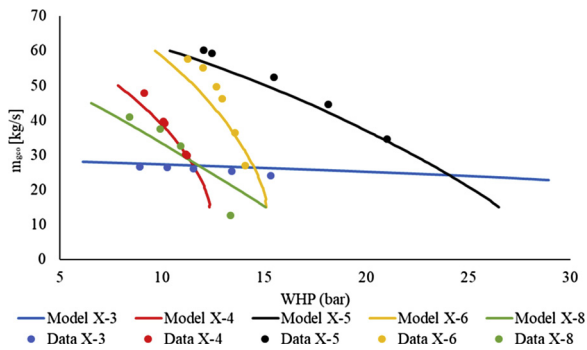


Fig. 3. Deliverability curves and data validation for the Sibayak field.

$$\begin{aligned}
 9 &\leq WHP_A \leq 15 \\
 9 &\leq WHP_B \leq 13 \\
 4.5 &\leq P_{sep} \leq 7.5 \\
 0 &\leq x_{R601} \leq 1
 \end{aligned} \tag{13}$$

The upper limits of WHP_A and WHP_B are determined based on the production well simulation results, where the maximum operating pressure of Well A and Well B are 15 bar and 13 bar, respectively. The lower limit of WHP_A and WHP_B is determined from the upper limit of P_{sep} . The genetic algorithm (GA) method is applied in the optimization process with the MATLAB optimization toolbox due to GA could find the real global optima value not the pseudo-optimal value and refer to previous study carried out by (Zhao and Wang, 2016; Mokarram and Mosaffa, 2018). Optimization using the GA method is conducted for 100 generations, with a population size of 100 individuals, a crossover probability of 0.95, and convergence of 95 %.

3. Results and discussion

3.1. Wellbore simulation and validation

The wells simulation generates the wells deliverability curves and data validation as shown in Fig. 3. The relative error from 5 wells are lower than 11 %. A very high reservoir pressure in the well X-3 area leads to stable production over a wide range of wellhead pressures, but the amount of geothermal fluid produced tends to be lower than other wells because its PI value is very low. Wells X-4 and X-6 have the same reservoir pressure, but the PI value of well X-6 is higher than well X-4, so for the same value of WHP , well X-6 produces more geothermal fluid. The explanation for wells X-5 and X-8 is the same as that for wells X-4 and X-6. From the curve, well X-5 is the best producing well owing to its high geothermal fluid production and wide WHP operating range.

3.2. Pipeline system

As it is stated before, this study considers the losses that occurred in

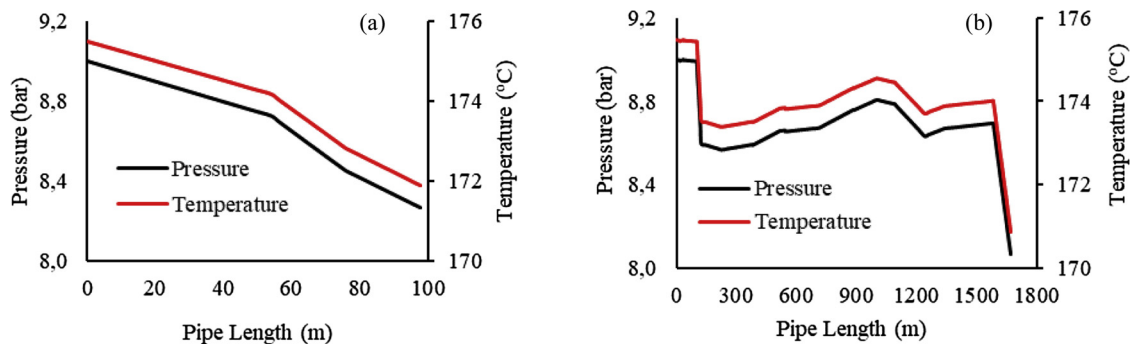


Fig. 4. Profile of geothermal fluid: (a) Well A pipeline; (b) Well B pipeline.

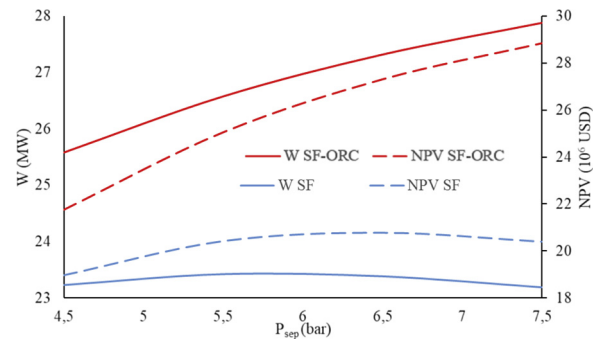


Fig. 5. Effect of P_{sep} on power output and NPV of SF and SF-ORC cycles.

the pipeline system. Fig. 4 shows the pressure profile of the geothermal fluid that flows through the pipelines from the wellhead to the power plant. For the Well A pipeline, the geothermal fluid pressure continues to decline from the wellhead to the power plant. This is caused by the increasing elevation from Well A to the power plant, so the geothermal fluid loses its energy to flow against gravity. For the Well B pipeline, the pressure of the geothermal fluid initially decreases, then rises at pipe lengths of $\sim 300\text{--}1000$ m and $1250\text{--}1600$ m. This is caused by the pipe elevation decreasing at those intervals, so the fluid receives more energy from gravity, which increases the fluid pressure. The elevation changes resulting pressure drop along the pipeline gives less specific enthalpy to the geothermal fluids when reaching the power plant, this leads to less power produce and less profit gained.

3.3. Thermo-economic analysis

Geothermal fluid that entered geothermal power plant is entering flash tank to separate liquid and gas. The pressure in the separator is a critical parameter to asses as Fig. 5 shows the effect of P_{sep} variations to the power produce and NPV in SF and SF-ORC. Both parameters are really depends on the P_{sep} . For SF, as the P_{sep} increases power produce and NPV are increased and after reaching certain point it is decreased. This is caused by increases in P_{sep} leads to increases in specific enthalpy of the saturated vapor and decreases in the mass flow rates. This phenomenon is caused by the changes of P_{sep} affecting the condition of the geothermal fluids in the separator. In higher P_{sep} , the fluids tends to form more liquid and in the lower P_{sep} the fluids tends to form more gas. This affects the mass flow rate of the saturated vapor leaving the separator, since the higher the P_{sep} the lower the mass flow rate leaving the separator. Meanwhile, increasing P_{sep} tends to lower the quantity of the vapor but, it increases the specific enthalpy of the vapor. Since the power produce from the SF depends not only from the quantity but also the quality (specific enthalpy) of the vapor, thus the power produce function of P_{sep} has a trade-off due to this contradictory phenomenon. This trade-off not only affecting power produce but also SF's NPV although from the Fig. 5 it can be seen that it has a lower impact in NPV

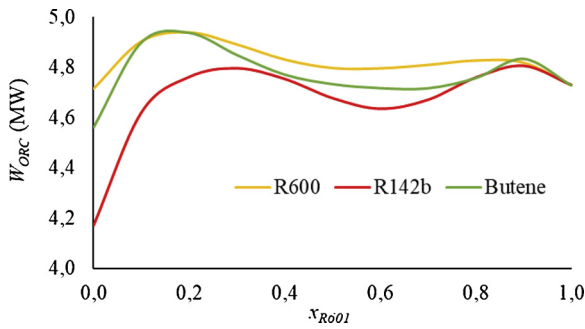


Fig. 6. Effect of x_{R601} on power output of ORC.

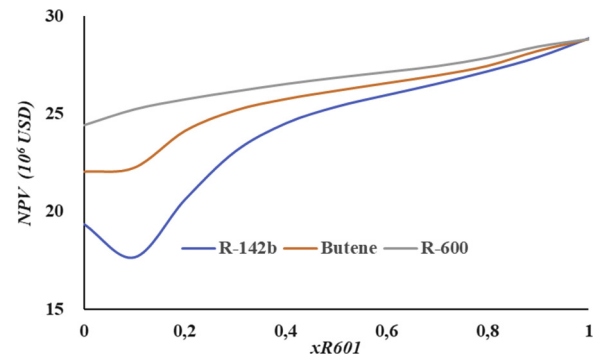


Fig. 8. Effect of x_{R601} on NPV of SF-ORC.

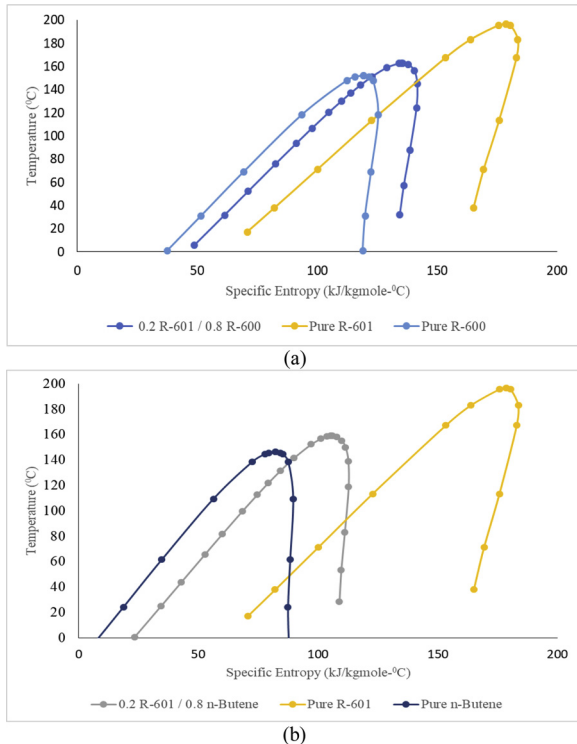


Fig. 7. T-s Diagram (a) R-601 and R-600, (b) R-601 and n-butene.

due to the fact that higher P_{sep} makes the specific volume of the vapor decreases therefore, the separator requires less volume that eventually requires less investment cost.

The trade-off that occurs in the SF does not happen in the SF-ORC. While, the SF depends on the vapor to produce electricity, SF-ORC can utilize the vapor and liquid leaving the separator. This leads to SF-ORC does not has a trade-off. Therefore the higher the P_{Sep} the higher the power produce from SF-ORC, and so does the NPV.

In the ORC, composition of the zeotropic mixtures play a significant role in determining the performance of ORC. Fig. 6 shows the effect of x_{R601} in the mixed working fluids R600/R601, R142b/R601, and butene/R601 on the power output of the ORC system. It shows that zeotropic mixture working fluids tend to give higher power output than the pure fluids, this result is in accordance with the works of Kolahi et al. (2018). This is because of the different working fluid mass flowrate. Fig. 7 shows the T-s diagram of optimized composition of zeotropic mixture used in working fluid and its pure component. Fig. 7 shows that zeotropic mixture has lower envelope at the same evaporator working temperature, 130 °C. This implies the lower latent heat required to evaporate the working fluid into saturated vapor. Because of the constant brine heat supply and the temperature of brine leaving the evaporator is set, it causes higher working fluid mass flow rate and leads to

higher power produce from ORC. However, in Fig. 7 shows that the secondary component, pure R-600 and butene, has lower envelop but lower power output, as shown in Fig. 6, compare to the zeotropic mixture. It is because zeotropic mixture has higher higher enthalpy. It leads higher power produced. Therefore, secondary pure component has higher mass flow but lower specific enthalpy hence resulting lower power produced.

Fig. 8 shows that the maximum NPV is obtained when the ORC working fluid used is pure R601. The effect of the temperature glide causes the zeotropic mixtures need higher evaporation and condensation pressure than pure R601 and thus, decreases the log mean temperature difference (LMTD) of those heat exchangers. Consequently, additional investment is required owing to the larger heat transfer area needed. Although the power output obtained from zeotropic mixtures is higher than from pure R601 for a certain value of x_{R601} , the additional investment costs are higher than the additional revenue generated due to the increasing power output. Hence, the NPV of zeotropic mixtures is lower than the pure R601.

Figs. 9 and 10 show Grassmann diagrams for the SF cycle in the Sibayak geothermal field and the proposed SF-ORC cycle that has been optimized to achieve maximum NPV. The total exergy input to the system is estimated to be ~70.40 MW and the amount of electricity produced from the SF and SF-ORC cycles is 23.5 and 27.88 MW, respectively. The addition of the ORC as the bottoming cycle in the SF cycle reduce the exergy loss from an underutilized brine from 30.65 % to 17.85 %. Moreover, the addition of the ORC increases the thermal efficiency (η_{th}) and exergy efficiency (η_{ex}) from 8.47 % to 10.05 % and 33.37%–39.60%, respectively. From an economic aspect, utilization of the ORC increases the NPV of the cycle from USD 21,165,331 to USD 29,224,825.

3.4. Optimization

The results of optimization show that a flash–binary cycle with pure R601 as the ORC working fluid yields the maximum NPV (USD 29,224,825), while the maximum power output (28.09 MW) is obtained when the working fluid used in the ORC is a zeotropic mixture.

In zeotropic mixtures, evaporation and condensation pressures are higher than those of pure R601, so the investment cost of the evaporator and condenser for an ORC with zeotropic mixtures is higher than that for an ORC with pure R601. Although the electricity generated is greater, it is not as much as the investment costs incurred, therefore the NPV decreases. Fig. 11 shows a comparison of the investment cost of equipment in the ORC system that uses pure R601 and zeotropic mixtures as a working fluid under optimum conditions (Table 4).

3.5. Effect of the pipelines on system performance

Table 5 shows the pipelines effect on power output and NPV of the

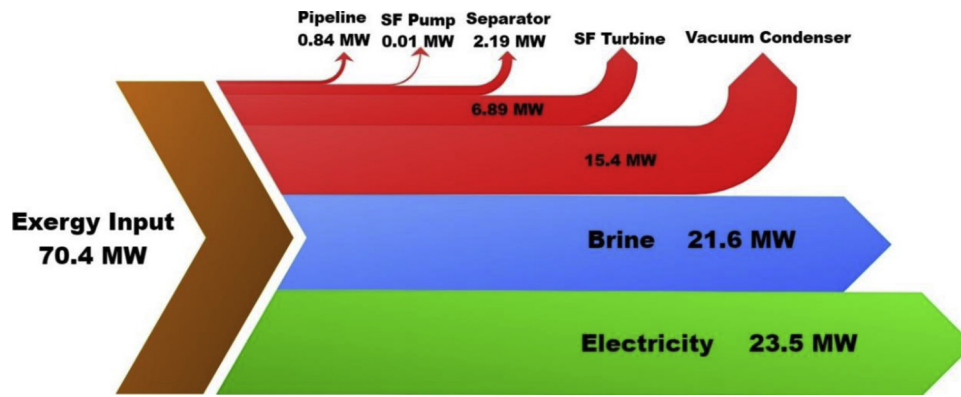


Fig. 9. Grassmann diagram of SF cycle at Sibayak.

system. The power outputs of a single-flash system and an ORC system considering pipelines' pressure drop are 23.4 and 4.48 MW, respectively. Meanwhile the power outputs for the system without considering the pipelines' pressure drop are 23 and 5.41 MW, respectively. When the pipelines omitted, P_{sep} is equal to WHP , the power output and NPV of the system without pipelines are 1.9 % (0.53 MW) and 9.9 % (USD 2,919,011) higher than those of a system with pipelines, respectively. For the system without pipelines, the higher power output is caused by higher P_{sep} giving more energy to the SF-ORC system. Therefore, the losses in pipeline that is usually omitted is 0.53 MW and it is equal to 0.23 Cents per kWh overestimation electricity price.

4. Conclusions

In this study, the utilization of ORC as the bottoming cycle increase the NPV, power output, energy efficiency, and exergy efficiency by USD 8,059,494; 4.38 MW; 1.58 %; 6,73 %, respectively, due to the reduction of the exergy loss from the underutilized brine. The maximum NPV was produced with the use of pure R601, while the zeotropic mixture resulting in the maximum power output. Considering the pipelines' pressure drop reduce the power output by 1.9 % and increase the NPV by 9.7 % compared to the system without pipelines' pressure drop. Moreover, a system without considering the pipelines' pressure drop overestimates the electricity price by 0.23 Cents per kWh.

Declaration of Competing Interest

The authors declare that there are no conflicts of interest.

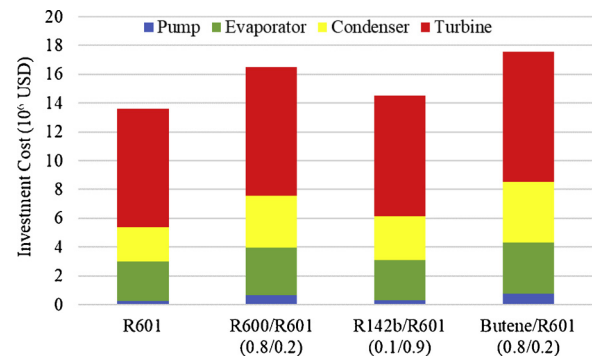


Fig. 11. Investment cost of equipment in ORC under optimum conditions.

Table 4 Optimization results of maximum NPV and power output.

Parameter	Maximum NPV	Maximum power output		
	Pure R601	R600/R601	R142b/R601	Butene/R601
WHP_A (bar)	9.0	9.0	9.0	9.0
WHP_B (bar)	9.0	9.0	9.0	9.0
P_{sep} (bar)	7.5	7.5	7.5	7.5
x_{R601}	1.0	0.2	0.9	0.2
NPV (USD)	29,224,825	25,730,842	27,909,574	24,444,055
W_{Net} (MW)	27.88	28.09	27.96	28.09
η_{th} (%)	10.05	10.14	10.09	10.14

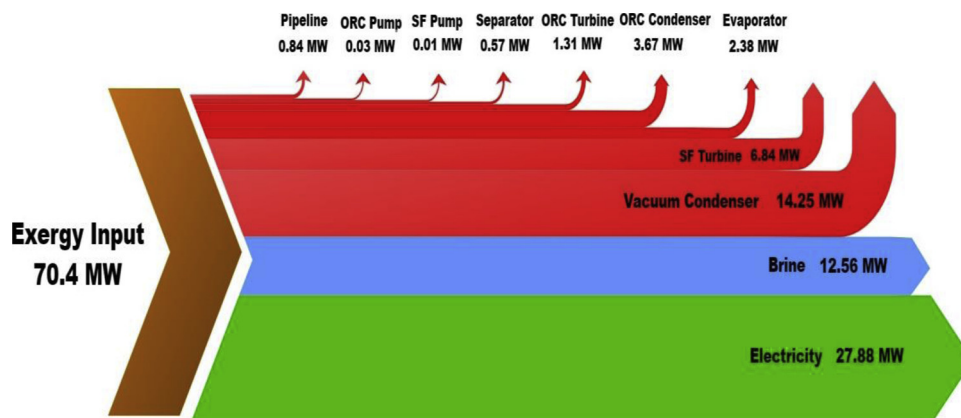


Fig. 10. Grassmann diagram of proposed SF-ORC cycle.

Table 5
Effect of pipelines on system performance.

System	WHP	P_{sep}	W_{Net} (MW)	NPV (USD)
With pipeline system	9.0	7.5	27.88	29,224,825
Without pipeline system	9.0	9.0	28.41	32,143,836

Acknowledgments

The authors are grateful to DRPM UI for supporting this work financially under the “Hibah Publikasi Artikel di Jurnal Internasional Kuartil Q1 dan Q2 (Q1Q2),” Contract Number NKB-0328/UN2.R3.1/HKP.05.00/2019.

Appendix A. Supplementary data

Supplementary material related to this article can be found, in the online version, at doi:<https://doi.org/10.1016/j.geothermics.2019.101778>.

References

- Aali, A., Pourmahmoud, N., Zare, V., 2017. Exergoeconomic analysis and multi-objective optimization of a novel combined flash-binary cycle for Sabalan geothermal power plant in Iran. *Energy Convers. Manage.* 143, 377–390.
- Atmojo, J., Itoi, R., Tanaka, T., Fukuda, M., 2019. Modeling Studies of Sibayak Geothermal Reservoir, Northern Sumatra, Indonesia.
- Edrisi, B.H., Michaelides, E.E., 2013. Effect of the working fluid on the optimum work of binary-flashing geothermal power plants. *Energy* 50, 389–394.
- Forecasts, M.W., 2019. Sibayak Weather Forecast, Indonesia [Online]. Mountain Weather Forecasts. Available: <https://www.mountain-forecast.com/peaks/Sibayak/forecasts/2212> [Accessed 23 June 2019].
- Ghasemian, E., Ehyaei, M.A., 2018. Evaluation and optimization of organic Rankine cycle (ORC) with algorithms NSGA-II, MOPSO, and MOEA for eight coolant fluids. *Int. J. Energy Environ. Eng.* 9, 39–57.
- Jalilinasrabady, S., Itoi, R., Valdimarsson, P., Saevarsdottir, G., Fujii, H., 2012. Flash cycle optimization of Sabalan geothermal power plant employing exergy concept. *Geothermics*.
- Kolahi, M.-R., Nemat, A., Yari, M., 2018. Performance optimization and improvement of a flash-binary geothermal power plant using zeotropic mixtures with PSO algorithm. *Geothermics* 74, 45–56.
- Leveni, M., Manfrida, G., Cozzolino, R., Mendecka, B., 2019. Energy and exergy analysis of cold and power production from the geothermal reservoir of Torre Alfina. *Energy* 180, 807–818.
- Lukawski, M.Z., Anderson, B.J., Augustine, C., Capuano, L.E., Beckers, K.F., Livesay, B., Tester, J.W., 2014. Cost analysis of oil, gas, and geothermal well drilling. *J. Pet. Sci. Eng.* 118, 1–14.
- Minoli, F., Snaidero, M., Frassinetti, M., 2017. Selection criteria of optimal separation pressure of liquid dominated geothermal resources. *Energy Procedia* 129, 629–636.
- Mohammadzadeh Bina, S., Jalilinasrabady, S., Fujii, H., Pambudi, N.A., 2018. Classification of geothermal resources in Indonesia by applying exergy concept. *Renew. Sustain. Energy Rev.* 93, 499–506.
- Mokarram, N.H., Mosaffa, A.H., 2018. A comparative study and optimization of enhanced integrated geothermal flash and Kalina cycles: a thermoeconomic assessment. *Energy* 162, 111–125.
- Oyewunmi, O.A., Ferré-Serres, S., Lecompte, S., Van Den Broek, M., De Paepe, M., Markides, C.N., 2017. An assessment of subcritical and trans-critical organic rankine cycles for waste-heat recovery. *Energy Procedia* 105, 1870–1876.
- Pambudi, N.A., 2018. Geothermal power generation in Indonesia, a country within the ring of fire: current status, future development and policy. *Renew. Sustain. Energy Rev.* 81, 2893–2901.
- Pambudi, N.A., Itoi, R., Jalilinasrabady, S., Gürtürk, M., 2018. Sustainability of geothermal power plant combined with thermodynamic and silica scaling model. *Geothermics* 71, 108–117.
- Pambudi, N.A., Itoi, R., Jalilinasrabady, S., Jaelani, K., 2014. Exergy analysis and optimization of Dieng single-flash geothermal power plant. *Energy Convers. Manage.* 78, 405–411.
- Pasek, A.D., Fauzi Soelaiman, T.A., Gunawan, C., 2011. Thermodynamics study of flash-binary cycle in geothermal power plant. *Renew. Sustain. Energy Rev.* 15, 5218–5223.
- Prananto, L.A., Zaini, I.N., Mahendranata, B.I., Juangsa, F.B., Aziz, M., Soelaiman, T.A.F., 2018. Use of the Kalina cycle as a bottoming cycle in a geothermal power plant: case study of the Wayang Windu geothermal power plant. *Appl. Therm. Eng.* 132, 686–696.
- Putra, A., Purwanto, W.W., Daud, Y., 2014. Pemodelan dan analisis sensitivitas reservoir geothermal lapangan x untuk estimasi potensi sumber panas. Undergraduate, Universitas Indonesia.
- Quinlivan, P., Assessment of Current Costs of Geothermal Power Generation in New Zealand, 2007. Australian Geothermal Energy Conference 2009 New Zealand. Sinclair Knight Merz. Basis.
- Seider, W.D., 2004. *Product and Process Design Principles: Synthesis, Analysis, and Evaluation*, second edition. Wiley, New York 2004 ©2004.
- Shokati, N., Ranjbar, F., Yari, M., 2015. Exergoeconomic analysis and optimization of basic, dual-pressure and dual-fluid ORCs and Kalina geothermal power plants: a comparative study. *Renew. Energy* 83, 527–542.
- Sinaga, R., Manik, Y., 2018. Optimizing the utility power of a geothermal power plant using variable frequency Drive (VFD) (case study: Sibayak geothermal power plant). *IOP Conference Series: Earth and Environmental Science* 124, 012007.
- Siregar, P.H.H., 2004. Optimization of Electrical Power Production Process for the Sibayak Geothermal Field. Geothermal Training in Iceland, Indonesia, pp. 349–376 2004.
- Su, W., Hwang, Y., Deng, S., Zhao, L., Zhao, D., 2018. Thermodynamic performance comparison of Organic Rankine Cycle between zeotropic mixtures and pure fluids under open heat source. *Energy Convers. Manage.* 165, 720–737.
- Vankeirsbilck, I., Vanslambrouck, B., Gusev, S., De Paepe, M., 2011. Organic Rankine cycle as efficient alternative to steam cycle for small scale power generation. 8th International Conference on Heat Transfer, Fluid Mechanics and Thermodynamics, Proceedings 785–792.
- Wang, D., Ling, X., Peng, H., Liu, L., Tao, L., 2013a. Efficiency and optimal performance evaluation of organic Rankine cycle for low grade waste heat power generation. *Energy* 50, 343–352.
- Wang, D., Ling, X., Peng, H., Liu, L., Tao, L., 2013b. Efficiency and optimal performance evaluation of organic Rankine cycle for low grade waste heat power generation. *Energy* 50, 343–352.
- Wang, F., Deng, S., Zhao, J., Zhao, J., Yang, G., Yan, J., 2017. Integrating geothermal into coal-fired power plant with carbon capture: a comparative study with solar energy. *Energy Convers. Manage.* 148, 569–582.
- Yari, M., 2010. Exergetic analysis of various types of geothermal power plants. *Renew. Energy* 35, 112–121.
- Yilmaz, C., 2018. Thermoeconomic cost analysis and comparison of methodologies for dora II binary geothermal power plant. *Geothermics* 75, 48–57.
- Yunus Daud, J.P.A., Sudarman, Sayogi, Ushijima, Keisuke, 1999. Reservoir imaging of the Sibayak geothermal field, Indonesia using borehole-to-surface resistivity measurements. *Proceedings of the New Zealand Geothermal Workshop* 21, 139–144.
- Zare, V., Mahmoudi, S.M.S., 2015. A thermodynamic comparison between organic Rankine and Kalina cycles for waste heat recovery from the gas turbine-modular helium reactor. *Energy* 79, 398–406.
- Zarrouk, S.J., Purnanto, M.H., 2015. Geothermal steam-water separators: design overview. *Geothermics* 53, 236–254.
- Zeyghami, M., 2015. Performance analysis and binary working fluid selection of combined flash-binary geothermal cycle. *Energy* 88, 765–774.
- Zhao, Y., Wang, J., 2016. Exergoeconomic analysis and optimization of a flash-binary geothermal power system. *Appl. Energy* 179, 159–170.